Femtosecond spectroscopy of electron-electron and electron-phonon energy relaxation in Ag and Au

Groeneveld, R.H.M.; Sprik, R.; Lagendijk, A.

Link to publication

Femtosecond spectroscopy of electron-electron and electron-phonon energy relaxation in Ag and Au

Rogier H. M. Groeneveld* and Rudolf Sprik

*Van der Waals-Zeeman Laboratorium der Universiteit van Amsterdam,
Valckenierstraat 65-67, 1018 XE Amsterdam, The Netherlands*

Ad Lagendijk

*Van der Waals-Zeeman Laboratorium der Universiteit van Amsterdam,
Valckenierstraat 65-67, 1018 XE Amsterdam, The Netherlands
and Fundamenteel Onderzoek der Materie-Instituut voor Atoom-en Molecuulfysica,
Kruislaan 407, 1098 SJ Amsterdam, The Netherlands*

We show experimentally that the electron distribution of a laser-heated metal is a nonthermal distribution on the time scale of the electron-phonon (e-ph) energy relaxation time τ_E. We measured τ_E in 45-nm Ag and 30-nm Au thin films as a function of lattice temperature (T_i =10–300 K) and laser-energy density ($U_\ell = 0.3$–1.3 J cm^{-3}), combining femtosecond optical transient-reflection techniques with the surface-plasmon polariton resonance. The experimental effective e-ph energy relaxation time decreased from 710–530 fs and 830–530 fs for Ag and Au, respectively, when temperature is lowered from 300 to 10 K. At various temperatures we varied U_ℓ between 0.3–1.3 J cm^{-3} and observed that τ_E is independent from U_ℓ within the given range. The results were first compared to theoretical predictions of the two-temperature model (TTM). The TTM is the generally accepted model for e-ph energy relaxation and is based on the assumption that electrons and lattice can be described by two different time-dependent temperatures T_e and T_i, implying that the two subsystems each have a thermal distribution. The TTM predicts a quasiproportional relation between τ_E and T_i in the perturbative regime where τ_E is not affected by U_ℓ. Hence, it is shown that the measured dependencies of τ_E on lattice temperature and energy density are incompatible with the TTM. It is proven that the TTM assumption of a thermal electron distribution does not hold especially under our experimental conditions of low laser power and lattice temperature. The electron distribution is a nonthermal distribution on the picosecond time scale of e-ph energy relaxation. We developed a new model, the nonthermal electron model (NEM), in which we account for the (finite) electron-electron (e-e) and electron-phonon dynamics simultaneously. It is demonstrated that incomplete electron thermalization yields a slower e-ph energy relaxation in comparison to the thermalized limit. With the NEM we are able to give a consistent description of our data and obtain values for the e-e scattering rate $K = 0.10 \pm 0.05$ fs^{-1}eV^{-2} for Ag and Au and for the e-ph coupling $g_\infty = 3.5 \pm 0.5 \times 10^{16}$ Wm^{-3}K^{-1} for Ag and $3.0 \pm 0.5 \times 10^{16}$ Wm^{-3}K^{-1} for Au.

I. INTRODUCTION

The nonequilibrium dynamics of laser-heated conduction electrons in metals and superconductors is a fascinating area of intense research. Irradiating a metal by a sufficiently short laser pulse can lead to a significant (effective) temperature rise of the electrons with respect to the ionic lattice. Several elementary processes such as electron-electron (e-e) and electron-phonon (e-ph) collisions will participate in the formation of a new thermal equilibrium. These processes lie at the basis of a wide range of phenomena in solid state physics. Electron-phonon interactions are of major importance to the electrical and thermal transport in metals and govern the formation of the superconducting state. Electron-electron collisions have attracted renewed interest as a result of their key role in disordered metallic systems. Femtosecond spectroscopy enables us to gain insight into those elementary processes by monitoring the relaxation of laser-heated electrons and phonons directly in the time domain.

In femtosecond thermomodulation spectroscopy an ultrashort "pump" laser pulse heats up the sample. A second "probe" pulse is time delayed with respect to the pump pulse. Measuring the change of the probe reflectivity (or transmissivity) as a function of the time delay between pump and probe pulse maps out the cooling on a femtosecond time scale. The application of this simple technique has led to a wealth of new information. Transient reflection and transmission experiments have been performed on Au,[1] Cu,[2] Ag,[3] and various conventional[4] and high-T_c (Refs. 5, 6) superconductors. One of the great achievements obtained by the technique is the direct determination of the e-ph coupling constant, relevant to, e.g., the superconducting properties of the material.[7] Other dynamical relaxation channels have been uncovered such as the ballistic component in the electronic heat transport.[8] The role of nonequilibrium heating in relation

to the optical damage threshold was investigated[9] and effects of the lattice disorder on the energy relaxation have been seen.[10]

The nonequilibrium *within* the electron gas is a nearly unexplored type of dynamics and has recently drawn great interest.[11-15] In the interpretation of thermomodulation data it was generally assumed that the electron gas formed a thermal distribution within the pulse duration ($\sim$ 100 fs) with the argument that the e-e scattering time for electrons that are highly excited (2 eV) in the conduction band is very small ($\sim$ 10 fs). It has not been recognized until recently[11] that nonthermal effects are clearly observable, even on a picosecond time scale, when conditions of low laser excitation power and low temperature are chosen. Under these circumstances, the e-e collision rate becomes strongly suppressed as a result of the Pauli exclusion principle reducing the phase space for e-e scattering. Our sensitive thermomodulation setup, based on the *surface-plasmon polariton* (SPP) resonance, enables us to measure under low-power and low-temperature conditions and thus provides the opportunity to observe e-e dynamical effects in metals.

In this paper we report on a detailed study of the e-ph energy relaxation process for thin Ag and Au films as a function of lattice temperature and deposited laser energy density. We observe a decrease of the effective relaxation time (from 710–530 fs and 830–530 fs for Ag and Au, respectively) when the temperature is lowered from 300 to 10 K. The relaxation time is found to be nearly independent from the deposited laser energy density within the range of 0.3–1.3 J cm^{-3}. The experimental results are compared to the *two-temperature model* (TTM), which is the commonly accepted theory to describe the energy relaxation dynamics between electrons and lattice and which is based on the same premises as the famous Bloch-Grüneisen law for the resistivity. We find large discrepancies between our experimental data and the TTM.

The discrepancies are resolved when we explicitly account for the finite e-e dynamics in a laser-heated metal. It will be shown that under our experimental conditions the excited electrons do not reach a thermal distribution on the time scale of the e-ph energy relaxation. We theoretically show that the incomplete thermalization makes the e-ph energy relaxation rate significantly slower below room temperature and nearly insensitive to the deposited laser-energy density, as compared to the thermalized limit. The presence of a nonthermal electron distribution is in contrast to the major assumption of the TTM. We introduce a new model, the *nonthermal electron model* (NEM), which is based on the Boltzmann equation accounting for both e-e and e-ph interactions simultaneously. With this model we are able to give a consistent representation of our measurements and obtain quantitative results for the e-e collision rate and the e-ph coupling strength. The measured values for the e-e collision rate compare well with other experimental and theoretical results.

Other groups have now found clear evidence of the finite e-e dynamics. Room-temperature measurements were made by femtosecond thermomodulation around the absorption edge on Au,[13] picosecond ultrasonics on Al,[14] and subpicosecond photoemission on Au (Ref. 12) and Cu(100).[15] The interpretation of these measurements involved a separate and sequential treatment of the e-e and e-ph channels. However, our theory accounts for the simultaneous action of both channels which is essential for a tightly coupled system.

Other groups have measured e-ph energy relaxation in various metals and seen dependences on temperature or laser energy density. In two room-temperature experiments[1,10] on Au an increase of the e-ph energy relaxation time has been seen upon increasing the laser fluence. However, the results were not interpreted in terms of the TTM. In the study of the e-ph relaxation dynamics of Nb as a function of temperature a decrease of the relaxation time has been observed when temperature was decreased.[16]

The presence of a transient nonthermal electron distribution has several implications. It is important in the correct interpretation of the thermomodulation data and the extraction of the e-ph coupling constant, as will be shown in this paper. In general, the study of degenerate electrons in metals will be beneficial to the understanding of relaxation phenomena in highly doped (10^{19} cm^{-3}) semiconductors. The presented technique is one of the few others (such as hot-electron transport[17] and low-temperature resistivity[18] measurements) by which we gain access to the the dynamical interactions within the conduction electrons of a metal.

Section II is devoted to the experimental technique and gives a short overview of the measurements. The measurements are interpreted using the TTM (Sec. II) and the NEM (Sec. III). Section III starts with a theoretical introduction to the TTM (Sec. III A), followed by the analysis of the experimental data (Sec. III B). In Sec. III B 1 we focus on the dependence on the lattice temperature, the dependence on the deposited laser energy density (Sec. III B 2), and the averaged e-ph energy relaxation time (Sec. III B 3). Concluding remarks on the TTM are made in Sec. III C. Section IV is devoted to the nonthermal electron model. In the introduction (Sec. IV A), the consequences of a nonthermal electron distribution for the e-ph relaxation process are qualitatively discussed. The NEM is formulated in Sec. IV B. The comparison between the experimental data and the NEM, made in Sec. IV C, results in experimental values for the e-e scattering rate for our samples. These values are compared in Sec. IV D to theoretical and experimental results which have been found by others. Conclusions are presented in Sec. V.

II. EXPERIMENTAL TECHNIQUES AND DATA

The use of the surface-plasmon polariton (SPP) resonance of metallic thin films and interfaces has been widely recognized as a powerful method of enhancing the electromagnetic field at surfaces.[19] Applications of the SPP resonance can be found in studies of, e.g., electronic[20] and vibrational[21] surface relaxation and surface second-harmonic generation.[22] In our experiment

the SPP resonance is combined with femtosecond pump-probe techniques. We heat and probe the electron gas by the excitation of SPP's. A SPP is a coupled surface mode of the electron gas and the electromagnetic field. In our case where the laser frequency (2 eV) is much lower than the surface-plasmon frequency (4.1 eV for Ag) the polariton has mainly photon character. We may regard the SPP as a photon, traveling along the metal-vacuum interface. The SPP's can easily be optically excited by the method of Kretschmann,[23] based on attenuated total reflection in a prism–metal-film–vacuum geometry. Resonant excitation of SPP's occurs when the laser beam is p polarized and internally reflected from the hypothenuse face of a transparent prism, on which the metal film of suitable thickness has been coated. At a critical angle of incidence, the SPP-resonance angle Φ_{SPP}, a sharp minimum in the reflectivity $R(\Phi)$ is found at which nearly all the light excites SPP's. The SPP's travel along the metal-vacuum interface and gradually decay due to the finite conductivity of the metal. The electric-field intensity of the SPP is concentrated at the metal-vacuum interface and decays exponentially into the metal with a penetration depth of ~ 12 nm. As the SPP decays, it creates hot electron-hole pairs that rapidly redistribute their energy in the Fermi sea via e-e collisions. Heat transport by the ballistic or diffusive motion of electrons occurs on a 20–50-fs time scale for our 30–50-nm thin films. The electrons emit or absorb phonons and exchange energy with the lattice. Through this aspect of the electron-phonon coupling, the heated electrons transfer energy to the lattice and cool. The characteristic time scale on which energy relaxation takes place is ≈ 700 fs for Ag at room temperature. The last relaxation step is the nanosecond-time-scale diffusion of heat out of the film into the prism.[24]

Not only does the SPP resonance provide an efficient way to excite electrons, it is also used to detect the small hot-electron-induced change of the complex dielectric constant $\Delta\epsilon$. The position, depth, and width of the reflectivity curve $R(\Phi)$ depend strongly on $\Delta\epsilon$. By tuning the probe angle to one of the two steep sides of $R(\Phi)$ [where $dR(\Phi)/d\Phi$ is extremal], a maximal sensitivity to the hot-electron-induced shift of Φ_{SPP} is attained. In most thermomodulation experiments the probe photon frequency lies close to the interband transition. In that case the thermal smearing of the Fermi level mainly causes a change of the absorption of the probe beam. In our case, the probe frequency (2 eV) lies far below the interband freqencies (Ag, 4 eV; Au, 2.5 eV).[25–27] For the latter condition it has been shown experimentally[3] that the Fermi smearing appears as a *dispersive* modulation at the probe frequency. This experimental result is explained theoretically in the Appendix, where it will be shown that $\Delta\epsilon$ is mainly real. Moreover, we show that it is proportional to the total excess *energy* contained in the electron gas, provided that the energy of individual excitations (electrons and holes) and the photon energy (2 eV) is much smaller than the energy of interband transitions. As this inequality holds at any time (> 150 fs) when measurements are performed, it is concluded that, by recording the change of reflectivity, the energy relax-
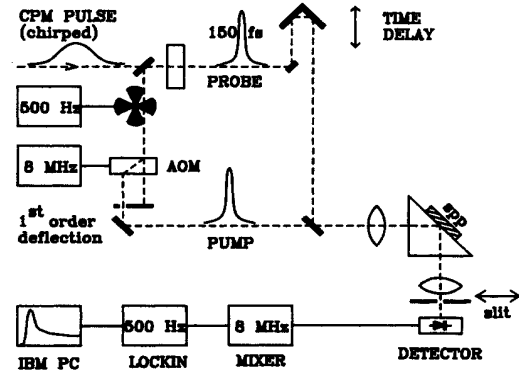
FIG. 1. Experimental pump-probe setup using the surface-plasmon polariton resonance of a metal film.

ation of the electron gas is measured.

The experimental setup[3] (see Fig. 1) is based on a colliding-pulse mode-locked (CPM) laser which delivers 150-fs pulses with a center wavelength of 630 nm (2 eV) at a repetition rate of 95 MHz. The laser beam is split in two. The pump beam is doubly amplitude modulated by an acousto-optic modulator (8 MHz) and a chopper (500 Hz). In this way the influence of noise is suppressed by the synchronous detection using a high-frequency mixer and lock-in amplifier. The weak probe beam passes a time delay stage. Both beams are focused onto the prism-metal interface under SPP-resonant conditions by a 50-mm focal-length achromatic lens to 20-μm-diam spots. The deposited laser energy density by the pump pulse is estimated to be $U_\ell = 1.3$ J cm^{-3}. The Ag films (45 nm thick) were evaporated on a substrate in a standard vacuum chamber at 10^{-6} torr. Under these circumstances the films are known[28] to be polycrystalline. The substrates were single-crystal, optically polished quartz plates, glued on the hypothenuse of a quartz prism. The 30-nm Au films were epitaxially grown in a molecular-beam epitaxy chamber on the freshly air-cleaved hypothenuse of a single-crystal NaCl prism. The crystallinity of the Au films was checked by reflection high-energy-electron diffraction (RHEED) during growth. The NaCl prism or the quartz plate was thermally anchored to the cold finger of a helium continuous-flow cryostat.

III. TWO-TEMPERATURE MODEL

In this part we will show that the generally accepted TTM fails to explain our experimental results. In the first section, the basic features of the TTM are outlined. A comparison of the experimental results and the calculated time dependence of the energy contents of electrons using the TTM is made. Next, a detailed analysis of the dependence of the measured deposited laser-energy density on the relaxation behavior is presented. It is shown that the temperature dependence in combination with the deposited energy dependence is in striking contrast to the predictions given by the TTM.

A. Theory

In this section we will outline the general features of the TTM. The metal is divided into two subsystems: the conduction electrons with a temperature T_e and the ionic lattice with a temperature T_i. The TTM describes the flow of heat between electrons and lattice which occurs when $T_e > T_i$ after laser excitation. The basic underlying assumption in the TTM is that the electron and phonon subsystems are each maintained in a thermalized state by (Coulombic) e-e and (anharmonic) ph-ph interaction, respectively. The time evolution of the energy (or temperature) of the electron gas and the lattice is given by two coupled heat equations[29]

$$C_e \frac{dT_e}{dt} = \nabla \cdot (\kappa_e \nabla T_e) - H(T_e, T_i) + P(t)$$

$$C_i \frac{dT_i}{dt} = +H(T_e, T_i). \tag{1}$$

Here, $P(t)$ is the amount of laser power (in W m^{-3}) that is dissipated in a unit volume of the electron gas and C_e and C_i are the specific heats of electrons and lattice, respectively. H is the energy transfer rate (in W m^{-3}) between electrons and lattice. The term $\nabla \cdot (\kappa_e \nabla T_e)$ describes the diffusive electronic heat transport out of the excited region.

We will make the following approximations. First, the electronic specific heat is given by $C_e = \frac{2}{3}\pi^2 \mathcal{N}(E_F)k_B^2 T_e \equiv \gamma T_e$, where $\mathcal{N}(E_F)$ is the density of states at the Fermi energy. Including the renormalization of the specific heat by the e-ph coupling would enhance the specific heat by a factor $(1 + \lambda)$ at temperatures $T_e \ll \Theta_D$. Here, Θ_D is the Debye temperature [= 210 (170) K for Ag (Au); see Ref. 30] and λ is the e-ph coupling parameter. For materials with a weak e-ph coupling such as Ag ($\lambda = 0.12$) and Au (0.15), we may neglect this factor.[7,31] Second, the electron temperature is assumed to be homogenous. Namely, the characteristic time scales for diffusive transport,[9] $\tau_d = C_e d^2/(2\kappa_e) = 50$ (30) fs, and ballistic transport, $\tau_b = d/v_F = 30$ (20) fs, for a 45- (30-) nm Ag (Au) film, are small compared to the laser pulse duration $t_p = 150$ fs [taking $\kappa_e = 420$ (310) W m^{-1} K^{-1}, $C_e = \gamma T_i$, $\gamma = 65$ (66) J m^{-3} K^{-2}, $T_i = 300$ K, and $v_F = 1.4$ (1.4) $\times$ 10^6 ms^{-1} for Ag (Au)]. In the latter argument we have taken into account the fact that the large ratio between laser spot diameter and film thickness causes the heat transport to be quasi-one-dimensional. Below room temperature the diffusive transport time will even decrease since the mean free path for scattering with phonons increases. Third, the rise of the lattice temperature may be neglected when calculating the electronic relaxation. Namely, the lattice specific heat C_i is a factor 100 larger than the electronic specific heat at room temperature and still 10 times larger at 8 K. In the fourth place, the steady-state lattice temperature rise at the focus of the laser beams is negligible. On the basis of the tabulated values[32] of the thermal conductivity of our crystalline substrates we derived that the relative temperature rise is less than 3%. This allows us to interpret the measured temperature of the thermometer as the lattice temperature. Finally, the lattice heat transport can be neglected since it occurs on a nanoseconds time scale. Hence, the heat equation becomes

$$\gamma T_e \frac{dT_e}{dt} = -H(T_e, T_i), \tag{2}$$

where T_i is now a parameter.

The energy transfer rate H has been calculated by Kaganov et al.[33] It is based on the same assumptions as the electrical resistivity law of Bloch and Grüneisen (related to the momentum relaxation). The energy transfer rate is a sum over all the elementary one-phonon absorption and emission processes, weighted with the energy transfer ($\pm$ phonon energy) per collision. The electrons and phonons have Fermi-Dirac and Bose-Einstein distributions, respectively. The acoustic phonon spectrum is described with the Debye model. The total transfer of energy per unit volume and per second from electrons to phonons is

$$H(T_e, T_i) = f(T_e) - f(T_i), \tag{3}$$

where

$$f(T) = 4g_\infty \left(\frac{T}{\theta_D}\right)^5 \int_0^{\frac{\theta_D}{T}} \frac{x^4}{e^x - 1}dx. \tag{4}$$

In the literature of femtosecond spectroscopy the constant g_∞ is called the *electron-phonon coupling constant* (in the literature also denoted by G). A useful quantity is the first derivative of the function $f(T)$ which we call the electron-phonon coupling function $g(T) \equiv df/dT$. For $T_i \ll \Theta_D$ the function $g(T_i)$ varies as T_i^4 and for $T_i \gtrsim \Theta_D$ the function $g(T_i)$ goes to the constant value g_∞. In the limit $T_e - T_i \ll T_i$, the energy transfer function H may be written as

$$H(T_e, T_i) = g(T_i)(T_e - T_i). \tag{5}$$

The TTM offers a description of the time evolution of the electronic temperature $T_e = T_e(t)$ and the energy $U_e = U_e(t) = \frac{1}{2}\gamma T_e(t)^2$. In order to make a comparison between the TTM and the experiment we define the *instantaneous energy relaxation time* by

$$\tau_E(T_e, T_i) \equiv \frac{U_e(\infty) - U_e}{(dU_e/dt)}$$

$$= \frac{\gamma(T_e^2 - T_i^2)}{2H(T_e, T_i)}, \tag{6}$$

where $U_e(\infty) \approx \frac{1}{2}\gamma T_i^2$. After the above introduction, the dependence of the e-ph energy relaxation time on lattice temperature and deposited laser energy density is discussed briefly.

The dependence on the lattice temperature T_i is demonstrated best in the low-excitation region, for which $\Delta T_e(0) = T_e(0) - T_i \ll T_i$. In this regime the electron-phonon energy relaxation time is

$$\tau_E(T_i) = \frac{\gamma T_i}{g(T_i)}. \tag{7}$$

The energy content of the electrons gas, $U_e(t)$, decays exponentially with the time constant $\tau_E(T_i)$. Going from a temperature T_i high above the Debye temperature to lower temperatures, the relaxation time first decreases linearly due to the decrease of the electronic specific heat $[g(T_i) \approx g_\infty]$. Below the Debye temperature, τ_E is expected to pass a minimum and rises again $\propto T_i^{-3}$ as a consequence of the dominating temperature dependence of the e-ph coupling $g(T_i)$. The temperature dependence of τ_E is depicted later in Fig. 6. The minimum of τ_E lies for Ag at ~ 60 K.

The role of the deposited laser energy density U_ℓ is important since it determines the peak electron temperature

$$T_e(0) = \left(T_i^2 + \frac{2U_\ell}{\gamma} \right)^{1/2}, \qquad (8)$$

assuming $t_p \ll \tau_E$. Let us consider the high-temperature limit $T_i \gtrsim \Theta_D$ of the initial energy relaxation time Eq. (6):

$$\tau_E(T_e(0), T_i) \approx \frac{\gamma[T_e(0) + T_i]}{2g_\infty}. \qquad (9)$$

At a constant lattice temperature, the initial energy relaxation time will thus increase when the initial electron temperature $T_e(0)$ or the energy density U_ℓ is increased. In our experiments a deposited laser energy density $U_\ell = 1.3$ J cm^{-3} yields an electronic temperature rise of $\Delta T_e = 61$ K at $T_i = 300$ K, which shows that the experiments are performed in the perturbative regime.

B. Analysis of the experimental results

The time-resolved measurements have been performed at a large number of different temperatures between 300 and 10 K and for different amounts of the laser fluence. Several raw scans on Ag at different temperatures are displayed in Fig. 2. Measurements on the power dependence will be presented later. The measured signal ($\Delta R \approx 10^{-4}$ with an accuracy better than 1%) shows a
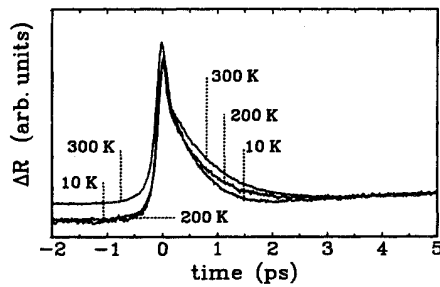
FIG. 2. Time-resolved measurements of the change of the reflectivity on Ag for various temperatures. The curves have been vertically shifted in order to let the plateau levels for $t > 4$ ps coincide and the vertical scales have been adjusted so that the peak signals are equal. It is seen that the subpicosecond relaxation speeds up as the temperature decreases.

sharp rise on the time scale of the pulse duration followed by a subpicosecond decay. Part of the signal around $t = 0$ is attributed to a coherence artifact of the pump and probe pulses. The decay is interpreted as the cooling of the electrons. It is seen that the relaxation speeds up as the temperature is lowered. The same phenomenon has been observed in Au. The measurements show the same trend as the quasilinear decrease of $\tau_E(T_i)$ in the TTM for $T_i > 50$ K. After a few picoseconds, a small contribution remains which is attributed to the heating of the lattice. For Au the lattice contribution reaches a constant value after several picoseconds. In the case of Ag, the lattice contribution appears to vary linearly within the time interval of 4–10 ps. This is due to an acoustic strain wave,[24] which bounces up and down in the film and results in a triangular pattern on $\Delta R(t)$ with a period of 25 ps. On the basis of this experimental fact we assume that the lattice contribution consists of a contribution proportional to the lattice temperature rise $\Delta T_i(t)$ due to the homogenous heating and a contribution proportional to $(at + b')\Delta T_i(t)$ due to the acoustic strain wave, where a and b' are constants. In most thermomodulation experiments, a linear relation between the electron temperature and the change of the dielectric constant (and hence ΔR) is taken, assuming that $\Delta T_e \ll T_e$ for all times. However, in the low-temperature regime this assumption may become invalid namely when $T_i \leq \sqrt{(2U_\ell/\gamma)}$ [see Eq. (8)]. When this assumption is not made and when probing Ag and Au with frequencies below the interband transition we are able to show that the hot-electron-induced change of the dielectric constant is proportional to the total excess energy $\propto \Delta T_e^2$ of electrons. This result is based on the theory of Rosei et al.[25–27] as elucidated in the Appendix and will be used in our interpretation. The total signal $\Delta R(t)$ is thus modeled by

$$\Delta R(t) \equiv \Delta R_i + \Delta R_e = (at + b)\Delta U_i(t) + c\Delta U_e(t), \qquad (10)$$

with $a, b,$ and c fitting parameters to be determined. We use the approximated coupled heat equations

$$\gamma T_e \frac{dT_e}{dt} = - g_{T_i}[T_e(t) - T_i(t)] + P(t)$$
$$C_i \frac{dT_i}{dt} = + g_{T_i}[T_e(t) - T_i(t)], \qquad (11)$$

where $T_i(0)$ is given by the thermometer temperature and where g_{T_i} and $T_e(0)$ are fitting parameters. From the experimental curve $\Delta R(t)$, the best fit is obtained for the five parameters a, b, c, g_{T_i}, and $T_e(0)$. The parameters g_{T_i} and $T_e(0)$ are decoupled from the lattice parameters a and b to a large extent, since a and b are predominantly determined by the data at large times > 4 ps whereas g_{T_i} and $T_e(0)$ are largely determined by the data in the time interval 0.25–4 ps. In Fig. 3 the fitted curve and the experimental data for $T_i = 180$ K have been plotted. The theoretical curve deviates less than 2% of the value of $\Delta R(0)$ from the measurement. This deviation is comparable to the measurement accuracy. The individual scans at a certain lattice temperature can be well fitted by a set of five fit parameters. However, the found fit values of $T_e(0)$ and g_{T_i} cannot be brought
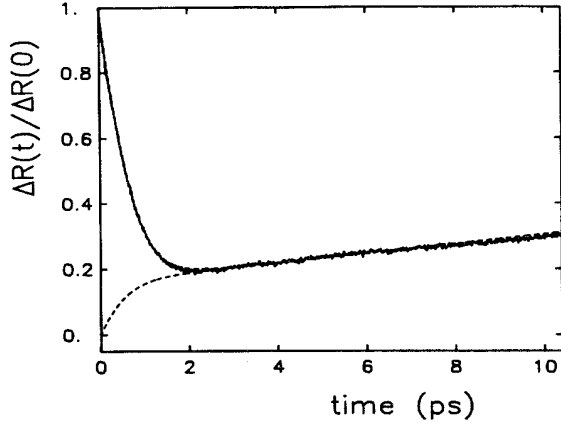
FIG. 3. Experimental time-resolved change of reflectivity of Ag at the substrate temperature of 180 K, together with a fit to the two-temperature model (TTM). In the fit to the TTM the lattice contribution is assumed to vary linearly in time between 4 and 10 ps. The dashed line shows the fitted lattice contribution. The fit of the sum of lattice and electron contribution overlaps with the measurement.

in accordance with the TTM. This will be shown in the following.

1. Dependence on the lattice temperature

In Fig. 4, we show a comparison of the measurements on Au and the TTM in the time domain. The regular subpicosecond oscillations on the measurements are an artifact. The measured change of the reflectivity of Au at 300 K has been used to derive the e-ph coupling constant $g_\infty = 2.6 \times 10^{16}$ W m^{-3} K^{-1} , which value is inserted in the TTM to obtain the time dependence of the electronic energy at 100 K for different amounts of the energy density. It is seen that the measurement at 100 K lies close to the 7.5-J cm^{-3} curve B, but differs greatly

from the 1.9-J cm^{-3} curve C. If curve B would be the correct description of the data, then a fourfold reduction of the laser power would have given curve C. However, in the next section it will be shown that the measurements were independent of the laser fluence, so that measurement curve $M2$ cannot be described by curve B. Using the full expression for the e-ph energy transfer [Eqs. (3) and (4)] does not lift the discrepancy.

2. Dependence on the deposited laser-energy density

We now turn to the dependence of the measurements upon the deposited laser-energy density. At a fixed temperature two time-resolved scans have been taken: a scan at normal pump power and a scan at an approximately fourfold reduced pump power. The reduction has been performed by electronically attenuating the laser beam deflection of the acousto-optic modulator. In this way the spatial and temporal beam alignments are best preserved. From the two time-resolved scans the following difference curve $D(t)$ is obtained:

$$D(t) = \frac{\Delta R(t, U_\ell) - a\Delta R(t, U_\ell/a)}{\Delta R(0, U_\ell)}, \qquad (12)$$

where $a \approx 4$. The difference $D(t)$ should vanish at all times when nonlinear effects are absent. The exact value of a has been determined by using the lattice contribution $\Delta R(t)$ for $t > 4$ ps as a linear energy-density meter: a is adjusted so that $D(t)$ is zero on the average for large times. In this way an extra simultaneous measurement of the doubly modulated pump power is avoided.

In Fig. 5 the difference curve $D(t)$ has been depicted for two scans on Ag at 180 K. Within a time of the pulse duration around zero delay time a considerable difference is present which is attributed to coherence effects. The e-ph relaxation occurs in the time interval 0.15–1 ps, in which interval the difference is less than 0.01. This experimentally found upper bound is much smaller than the difference as obtained from the TTM, which is maximal 0.04 for $U_\ell = 1.3$ J cm^{-1}. This procedure has been
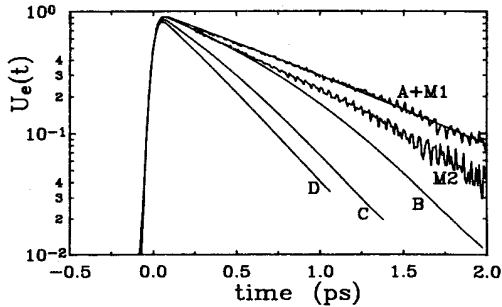

FIG. 4. Time-resolved measurements on Au at a lattice temperature of $M1$, 300 K, and $M2$, 100 K, compared to the energy $U_e(t)$ of the electrons in the two-temperature model at various deposited energy densities. Curve A: 300 K and 1.9 J cm^{-3}. Curves B, C, D at 100 K have 7.5, 1.9, and 0.5 J cm^{-3}, respectively. The regular subpicosecond oscillations on the measurements are an artefact.
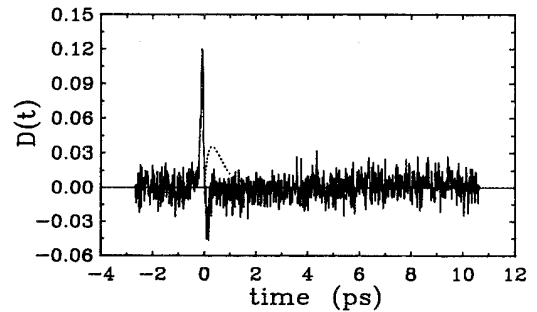

FIG. 5. Dependence of the measured change of reflectivity on the deposited laser-energy density U_ℓ on silver. The shown differences $D(t)$ should be zero when $\Delta R/R(t)$ depends linearly on U_ℓ. Lattice temperature $T_i = 180$ K. Solid line: experimental difference. Dashed line: difference given by the two-temperature model (TTM), at $U_\ell = 1.3$ J cm^{-1}.

repeated at different temperatures with the same result. We conclude that the measured change of the reflectivity shows a nonlinearity which is much smaller than the nonlinearity as predicted by the TTM.

3. Electron-phonon energy relaxation time

In order to combine the information on temperature and deposited laser-energy density dependence, a second representation of the measurements and the TTM is given in terms of the electron-phonon energy relaxation time. After subtracting the estimated lattice contributions, the data are represented by relaxation times averaged within the time interval 0.25–1.25 ps. The TTM is represented by the instantaneous electron-phonon energy relaxation time $\tau_E(T_e(0), T_i)$ taken at zero time[34] as a function of temperature. The calculation of $\tau_E(T_e(0), T_i)$, as defined by Eq. (6), accounts for the full energy transfer function $H(T_e, T_i)$. The function $\tau_E(T_e(0), T_i)$ has been drawn in Fig. 6 for different values of the energy density U_ℓ ranging from 0 up to 5.2 J cm^{-3} together with the average relaxation time of the measurements. For the sake of clarity the curves of finite U_ℓ have been drawn only in the high-temperature range [in which $\tau_E(U_2) > \tau_E(U_1)$ when $U_2 > U_1$ so that curves do not cross and the averaged e-ph energy relaxation time is meaningful]. The deposited laser energy is related to the peak electron temperature $T_e(0)$ by expression (8). At $T_i = 300$ K the relaxation time of the TTM can be made to match the corresponding experimental data point taking $g = 2.7 \times 10^{16}$ and 3.1×10^{16} W m^{-3} K^{-1} for Au and Ag, respectively. However, at lower temperatures a significant discrepancy arises: The experimental slope of the relaxation time versus T_i is 2–3 times smaller than predicted by the TTM. One might argue that the deposited energy must have been higher at low temperatures so that the slope is effectively decreased, but in that case we should have observed a large (30%) decrease in the relaxation time upon a (4 ×) reduction of the laser energy. In the previous section it was shown that this is not the case. For instance, the measurement on Ag at 180 K should, on the basis of the previous section, have had a relaxation time which lies below line B of Fig. 6(a). Both the observed *small slope* and the *independence* from laser energy are in striking contradiction with the TTM.

C. Conclusions to the TTM

We have sought several explanations for the observed discrepancies within the framework of TTM. First, we found that part of the measured data could be represented by TTM if a substantially larger Debye temperature (~ 400 K for Ag) was chosen. However, this is unrealistic with respect to the obtained values from heat capacity [210 K (Ref. 30)] or resistivity [230 K (Ref. 35)] measurements.

Second, we considered the fact that the acoustic strain wave in the case of Ag may indicate that a small spatial
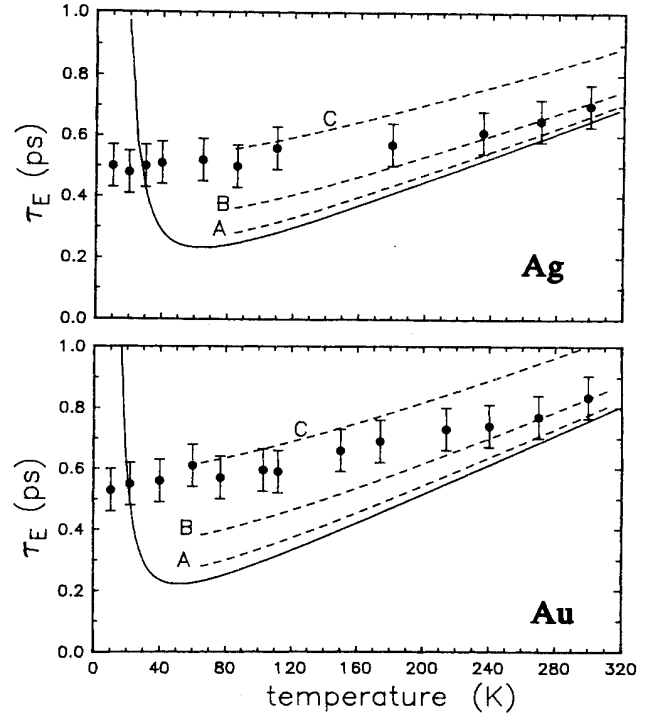

FIG. 6. Comparison between experimental data and the calculated electron-phonon energy relaxation time τ_E in the two-temperature model versus temperature for various amounts of deposited laser-energy density U_ℓ for Ag and Au. Solid line: infinitesimally small U_ℓ. Dashed lines A, B, C: $U_\ell = 0.3$, 1.3, 5.2 J cm^{-3}, respectively. Dots: experimental data. For the sake of clarity the curves of finite U_ℓ have been plotted in a limited temperature interval.

inhomogeneity in the electron distribution is still left after the pump pulse. Calculations show that this does not seriously affect the relaxation.

Third, possible effects of lattice disorder are discussed. It is known[36,37] that the presence of disorder enhances the low-energy part of the phonon density of states. The electron-phonon coupling is modified[38] for phonon wavelengths of the order of the elastic mean free path ℓ. We performed experiments on samples with a nearly crystalline structure. The Ag films have a residual resistance of 0.8 $\mu\Omega$ cm, corresponding to an elastic mean free path ℓ of 1200 Å. The estimated energy range below which the phonon density of states would be modified by the disorder $(hc_s/[\ell k_B] \approx 1$ K) lies far below the phonon energies which are relevant to our experiment. The resistivity at room temperature amounted to 2.4 $\mu\Omega$ cm, which lies close to the crystalline bulk value. Even a low-temperature correction is of no importance to the discussion of our data. We addressed the discrepancy between our experimental data and the two-temperature model which already occurs in the high-temperature $(T_i \gtrsim \Theta_D)$, quasilinear part of τ_E. In this regime quantities like resistivity, collision rate, and energy relaxation are not sensitive to details in the phonon spectrum. We conclude that the effects of disorder are negligible in our weakly disordered films.

The observed discrepancies are readily resolved when the dynamics within the electron system is incorporated in the relaxation model. This is accomplished in the next part.

IV. NONTHERMAL ELECTRON MODEL

A. Introduction

In this part it will be shown that e-e dynamics in a laser-heated metal plays an essential role in the e-ph relaxation on the picosecond time scale. Before presenting the full model in the next sections, we will discuss its role qualitatively.

Here, we will deal with the fact that the electron distribution in a metal, which has been irradiated by a femtosecond laser pulse, has excited electron-hole pairs with energies up to the photon energy (2 eV). This energy is much larger than the typical energies ($\sim 10^{-2}$ eV) the electrons would have in a thermal nonequilibrium distribution. For quasiparticles with energies $\varepsilon \equiv E - E_F$ close to the Fermi energy E_F, the interactions within the degenerate electron gas are well described by Fermi liquid theory. One of its results is the quasiparticle lifetime of an electron with energy ε interacting with electrons having a Fermi distribution of temperature T,

$$\frac{1}{\tau_{e\text{-}e}} = K \frac{(\pi k_B T)^2 + \varepsilon^2}{1 + \exp[-\varepsilon/(k_B T)]}. \quad (13)$$

Here, the quantity $K \equiv m^3/(8\pi^4\hbar^6)W_{e\text{-}e}$ is the characteristic e-e scattering constant that contains the angular-averaged scattering probability $W_{e\text{-}e}$. An alternative way of characterizing the e-e interaction[39] is by means of the energy $\bar{\varepsilon} = (\hbar K)^{-1}$. The characteristic energy $\bar{\varepsilon}$ is the cutoff energy above which the quasiparticle is not a well-defined eigenmode of the electron system. For highly excited electrons which have $\varepsilon \gg k_B T$ the quasiparticle lifetime reduces to

$$\tau_{e\text{-}e}^{-1} = K\varepsilon^2. \quad (14)$$

The evolution of the distribution function under e-e quasiparticle scattering events is strongly influenced by the Pauli exclusion principle. Let us consider the process of thermalization of a quasiparticle at energy ϵ (relative to the Fermi energy). In a collision with a "cold" electron from the Fermi sea it will share a large fraction of its energy. We approximate the e-e energy relaxation time by the quasiparticle lifetime at $T = 0$ and describe the energy loss of a single quasiparticle by

$$\frac{d\varepsilon}{dt} = -\frac{\varepsilon}{\tau_{e\text{-}e}}. \quad (15)$$

The "partial thermalization time" t_{th} for an electron to cool from the initial energy $\varepsilon(0)$ down to the energy ε is equal to

$$t_{\text{th}} \equiv t(\varepsilon) = \frac{1}{2K}\left(\frac{1}{\varepsilon^2} - \frac{1}{\varepsilon(0)^2}\right) \quad (16)$$

(see also Quinn[40]). The approximate time to reach for instance a 400-K thermalized distribution is $t_{\text{th}} \approx 1/(2Kk_B^2T^2) = 1.4$ ps, where we have taken $K = 0.3$ fs^{-1} eV^{-2} . This time is already twice as long as the typical e-ph energy relaxation time. It is concluded that the electron gas will not have reached a thermal distribution long before the e-ph energy relaxation process sets in. Notice that the first high-energy steps of thermalization occur very rapidly but slow down as more energy has been shared and the average electron energy moves towards the Fermi level. During the thermalization the number of quasiparticles (hot electrons) in the excess distribution grows exponentially.

What will be the consequence of a nonthermal electron distribution on the rate at which electrons lose their excess energy by the electron-phonon interaction? We adopt the above model and follow the quasiparticles in time against a zero-temperature Fermi sea. The total electronic energy of the electron gas will mainly decrease by spontaneous phonon emission. Since the average electron energy in the excess distribution is much larger than the width of the phonon spectrum during the e-ph energy relaxation, each electron in the excess distribution has a constant phonon emission rate named W. The amount of phonon-emitting electrons $n(t)$ is roughly doubled in each step of thermalization. Therefore, the energy relaxation rate $\propto Wn(t)$ to the lattice increases as the thermalization within the electron gas progresses. Reversing the argument it is concluded that incomplete thermalization reduces the e-ph energy relaxation rate of laser-heated electrons. Based on these ideas we developed a fully quantitative model for e-ph energy relaxation, the *nonthermal electron model*.

B. Theory

We consider a nonthermal electron gas coupled to the phonon system and calculate the energy loss to the lattice during thermalization. The Boltzmann equation describes the evolution of the electron distribution in time and contains a two-particle e-e collision integral and a one-phonon one-electron e-ph collision integral:

$$\frac{dn_\varepsilon}{dt} = \mathcal{C}_{e\text{-}e}[n_\varepsilon] + \mathcal{C}_{e\text{-}ph}[n_\varepsilon]. \quad (17)$$

The electron-electron collision integral $\mathcal{C}_{ee}[n_\varepsilon]$ is

$$\mathcal{C}_{e\text{-}e}[n_\varepsilon] = K \iiint dE_2 dE_3 dE_4 \delta(\varepsilon + E_2 - E_3 - E_4)$$
$$\times [n_3 n_4 (1 - n_\varepsilon)(1 - n_2)$$
$$- n_\varepsilon n_2 (1 - n_3)(1 - n_4)], \quad (18)$$

where $n_i = n(E_i)$. The separation of angular and energy variables, which enter the derivation of Eq. (18), is justified by the fact that the e-e interaction becomes largely isotropic due to screening by the other quasiparticles. Thus, screening is included to a first approximation. The electron-phonon collision integral is[41]

$$\mathcal{C}_{e\text{-ph}}[n_\varepsilon] = \frac{2^{\frac{3}{2}}\pi^2\hbar^3 g_\infty}{m^{\frac{3}{2}}k_B^2\Theta_D q_D^3} \int_0^{q_D} q^2 dq(\varepsilon + E_F)^{-\frac{1}{2}}$$
$$\times[n_{\varepsilon-u}(1 - n_\varepsilon)N_u - n_\varepsilon(1 - n_{\varepsilon-u})(1 + N_u)$$
$$+n_{\varepsilon+u}(1 - n_\varepsilon)(1 + N_u) - n_\varepsilon(1 - n_{\varepsilon+u})N_u],$$

$$(19)$$

where $u \equiv \hbar\omega_q$ is the phonon energy. The phonons have a Debye spectrum characterized by a Debye temperature Θ_D and a Debye wave number q_D. The screening of the e-ph interaction by the presence of the electron gas has been accounted for by the Thomas-Fermi screening in the small-wave-number limit.[42] The above e-ph collision integral is identical to the expression used in the e-ph momentum relaxation (the Bloch-Grüneisen law of resistivity) or the e-ph energy transfer function H of the TTM.

We performed an extensive numerical calculation based on the Boltzmann equation. In the calculation a thermal phonon distribution with constant temperature T_i and an initially nonthermal electron distribution $n = n_{T_i} \pm \Delta n$ which consists of a Fermi distribution n_{T_i} at temperature T_i and a small Gaussian electron (and hole) distribution $\pm\Delta n(\varepsilon)$ centered at ± 0.3 eV are taken with a width of 0.05 eV. The chosen energy is high enough to mimic the distribution 150 fs after laser excitation. After a few collisions a new nonthermal distribution will have developed that bears no relation to the initial distribution. The results are independent of the choice of the initial mean energy of the excess distribution. The Boltzmann equation is solved by a fifth-order Runge-Kutta numerical integration. A cubic-spline interpolation scheme has been used to evaluate the e-ph collision integral. The electronic distribution is represented by a discrete set $\{n_{\varepsilon_j}\}$ of $j = 100$–200 values within a window of 1.0–1.4 eV around the Fermi energy. From the calculated distribution functions the excess energy $U_e(t) = \int \varepsilon n_\varepsilon(t)d\varepsilon$ has been calculated as a function of time.

C. Comparison between the NEM and experimental data

We will first separate the electronic contribution ΔR_e to the measured reflectivity curve $\Delta R(t)$ from the lattice contribution ΔR_i. At the basis of the NEM lies the fact that energy is conserved within the system of electrons and phonons between the time just after the pump pulse $t > 150$ fs and a several tens of picoseconds. In that time interval all (excess) electronic energy flows to the lattice so that $dU_e/dt = -dU_i/dt$ or $\Delta U_i(t) \equiv C_i\Delta T_i = U_e(0)-U_e(t)$. Eventually, lattice heat conduction drains the excess heat but this process has no consequence for the description on a picosecond time scale. Since the statement holds for the TTM of Eq. (11) as well, the found description of the experimental data by the fit Eq. (10) and (11) forms a good parametrization of the electronic and lattice contributions to the signal. In this way the comparison between the TTM and NEM is not hindered by possible systematic errors in the

determination of the lattice contribution. On the basis of the energy conservation the parametrized lattice contribution is subtracted from the experimental data. The obtained curve represents the electronic contribution and will be used in the following analysis of the NEM.

In Fig. 7 a comparison of the experimental and theoretical energy relaxation times averaged over the time interval 0.25–1.25 ps is depicted for different temperatures T_i and values of the e-e collision rate K. The calculations have been performed down to temperatures of 50 K. Below this temperature the accurate representation of the sharp Fermi edge led to a substantial increase of computer time. The influence of the e-e dynamics confirms the qualitative picture of the introductory section. The e-ph energy relaxation rate increases when the e-e collision rate is increased for a constant e-ph coupling g_∞. The consequences of the nonthermal distribution become much more important at lower temperatures. The theoretical results given in Fig. 7 were obtained for $U_\ell = 1$–5 J cm^{-3}. Varying U_ℓ in this range led to nearly identical results, in agreement with the experimentally found insensitivity of τ_E to U_ℓ. The experimental data can be fitted well with the electron-phonon coupling $g_\infty = 3.5 \pm 0.5 \times 10^{16}$ W m^{-3} K^{-1} for Ag and $g_\infty = 3.0 \pm 0.5 \times 10^{16}$ W m^{-3} K^{-1} for Au. The experimental values of the e-e scattering rate amounts to $K = 0.10 \pm 0.05$ fs^{-1} eV^{-2} for Ag and Au. In Fig. 8 the comparison between the calculated excess energy of electrons and the
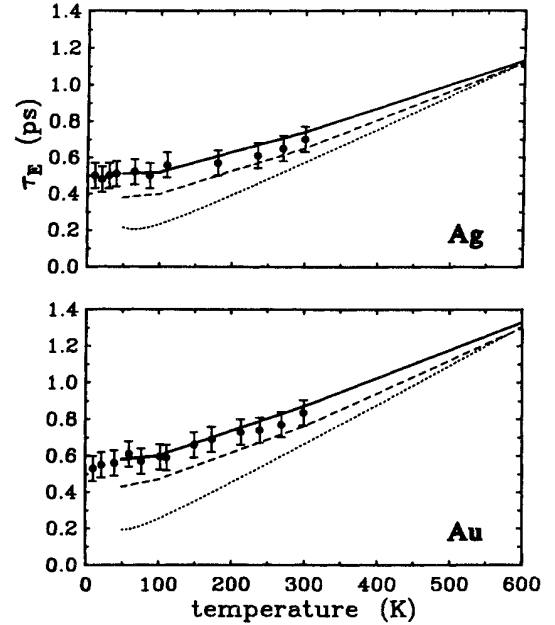

FIG. 7. Comparison between experimental data and the calculated average electron-phonon energy relaxation time τ_E using a Boltzmann equation that accounts for both electron-electron and electron-phonon scattering. Electron-electron scattering rate: solid line, $K = 0.1$ fs^{-2} eV^{-1}; long-dashed line, $K = 0.2$ fs^{-2} eV^{-1}; short-dashed line, $K = \infty$ (thermalized limit). For Ag and Au the electron-phonon coupling constant is $g_\infty = 3.5$ and 3.0×10^{16} W m^{-3} K^{-1}, respectively. Dots: experimental data.
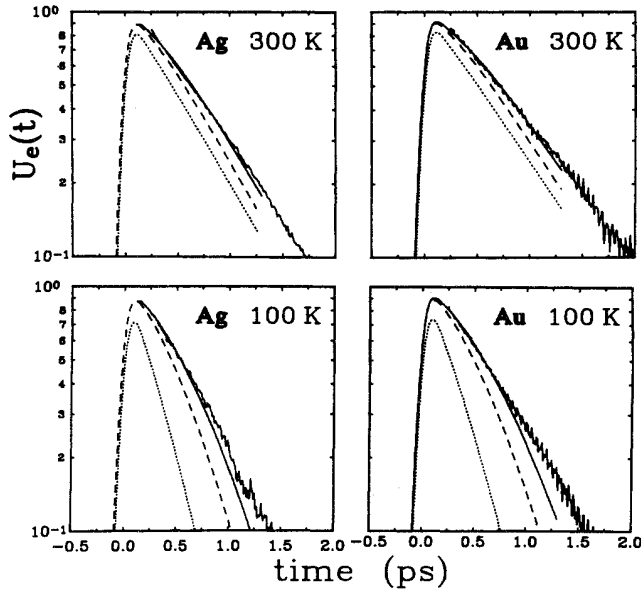
FIG. 8. Comparison between the measured time-resolved reflectivity and the excess energy $U_\ell(t)$ of electrons calculated with the Boltzmann equation incorporating electron-electron (e-e) and electron-phonon (e-ph) dynamics as a function of time at lattice temperatures of 100 K and 300 K. The e-e scattering rate: $K = 0.1$, 0.2 fs^{-2} eV^{-1} and $K = \infty$ for the solid, long-dashed, and short-dashed lines. For Ag and Au, the e-ph coupling is $g_\infty = 3.5$ and 3.0×10^{16} W m^{-3} K^{-1}, respectively. Energy density in the calculation, $U_\ell(0) = 1.9$ J cm^{-3}.

measurements representing the electronic contribution to the reflectivity as a function of time is displayed. The calculated curves are somewhat more nonexponential than the measured curves, but in general reproduce the measurements well. The important result of the NEM is that it is able to give a consistent picture of the e-ph energy relaxation time as a function of both lattice temperature and laser power.

The thermal excitations ($k_B T_i$) of quasiparticles enhance the e-e collision rate. This fact is elucidated by expression (13) of the quasiparticle lifetime at finite temperature T. The characteristic temperature $T_{e\text{-}e,e\text{-ph}}$ for which the thermally excited quasiparticles make the e-e collision time Eq. (13) equal to the e-ph energy relaxation time Eq. (7) is

$$T_{e\text{-}e,e\text{-ph}} = \left(\frac{g}{K \gamma \pi^2 k_B^2} \right)^{1/3}, \tag{20}$$

which is of the order of 300–600 K. Below $T_{e\text{-}e,e\text{-ph}}$, effects of e-e nonthermalization on the e-ph energy relaxation are present, as is clearly demonstrated by the calculations depicted in Fig. 7.

Comparing the dependence on the deposited laser energy density U_ℓ of the e-ph energy relaxation in the two models, we showed that the dependence is much weaker in NEM than in the TTM. Given a certain U_ℓ, electrons are dispersed within a characteristic energy win-

dow $0 < \varepsilon < \varepsilon_m$, where the characteristic energy ε_m for the TTM is $\sim k_B \sqrt{(T_i^2 + 2U_\ell/\gamma)}$, whereas ε_m for NEM is of the order of the photon energy $\hbar\omega$ and thus generally much higher. The change of occupation is larger for a smaller window. The relaxation rate is related to the occupation of levels within the window. Hence, the variation of the relaxation with U_ℓ will be larger in the TTM than in the NEM.

Refinements to the presented approach could still be made. In our calculation the e-ph and e-e scattering was assumed to be isotropic and basic screening models were incorporated. The influence of hot phonons and the resulting phonon-phonon dynamics remain to be investigated yet.

D. Comparison to other results

Several experimental and theoretical estimates for the e-e scattering rate are available. In all cases a linear relation is found between the scattering rate and the square of the energy difference $(E - E_F)^2$ for energies close to the Fermi energy.

The result of the calculation of the scattering rate by means of the random phase approximation[40,39] can be written as

$$K = \frac{\pi^2 \sqrt{3}}{128} \frac{\omega_p}{E_F^2} = 0.06 \text{ fs}^{-1} \text{ eV}^{-2} \quad \text{for Ag.} \tag{21}$$

In hot-electron transport measurements on metal-semiconductor thin-film structures,[17] it was found that electrons injected 0.83 (0.95) eV above the Fermi energy in Ag (Au) have mean free paths $\ell_{e\text{-}e}$ of 440 (360) Å, corresponding to $K = 0.04$ (0.05) fs^{-1} eV^{-2}. As a third estimate we quote the results of low-temperature ($<$4 K) resistivity measurements by Kaveh and Wiser.[18] They found a contribution $\rho(T)_{e\text{-}e} = A_{e\text{-}e}T^2$, with $A_{e\text{-}e} = 0.3$ (0.5) $\times 10^{-15}$ Ω m K^{-2} for Ag (Au). This contribution has been attributed to e-e umklapp scattering events. On theoretical grounds it was found that umklapp events form a large fraction $\Delta = 0.35$ of all scattering events. The resulting e-e scattering rate thus amounts $K = 2ne^2 A_{e\text{-}e}/(m\pi^2 k_B^2 \Delta) = 0.04$ (0.06) fs^{-1} eV^{-2} for Ag (Au). It is concluded that the e-e scattering rates deduced from our measurements are of the same order of magnitude as the quoted results.

As a conclusion to this section we will make a comparison between the e-e scattering rates of metals and semiconductors with degenerate carrier distributions. Recently, the carrier dynamics of high-carrier-density (10^{17}–10^{18} cm^{-3}) GaAs has been studied by time-resolved[43–45] and tunneling[46,47] experiments. In the latter experiments, a carrier-carrier scattering time of 50 fs for 250-meV electrons at a density of 10^{18} cm^{-3} in GaAs at 300 K has been found. The corresponding value $K = 0.3$ fs^{-1} eV^{-2} lies surprisingly close to typical values for metals. This can be understood considering the dimensionless parameter $r_s \equiv r_0/a_H$, where r_0 is the effective electron radius and a_H is the Bohr radius. Basic considerations lead to the fact that r_s is equal to the ratio of the Coulomb

interaction and the kinetic energy ($\approx E_F$) of electrons, so that r_s is directly related to the e-e scattering rate. For a degenerate density of 10^{18} cm^{-3} in n-type GaAs we find that $r_s = 0.6$. The value r_s differs only a factor of 5 from the metals Ag and Au having $r_s = 3$. The difference of more than six orders of magnitude in the density is partly compensated by the effective mass and the static screening. [In the estimate for GaAs we used $r_s = r_0/a_H^*$, where $a_H^* = a_H \epsilon m_0/m_e^*$ is the effective Bohr radius. The effective Bohr radius in GaAs is much larger (100 Å) than the bare radius (0.52 Å) as a result of the relatively small effective electron mass $m_e^* = 0.07 m_0$ in the Γ band and the large static dielectric constant $\epsilon = 13.18$.] The e-e dynamics in metals shows a large similarity with the carrier-carrier dynamics in high-carrier-density semiconductors in spite of the huge difference in the carrier density. The example stresses the relevance of time-resolved experiments on metals to the field of semiconductor physics.

V. CONCLUSIONS

We have performed femtosecond transient-reflection measurements in Ag and Au thin films by using the the surface-plasmon polariton resonance. This technique distinguishes itself from other femtosecond techniques by its capability to detect *small* transient changes in the energy content of the electron gas. With this method we have studied the dependence of the e-ph energy relaxation time τ_E on the lattice temperature and the laser fluence. The e-ph energy relaxation time decreases monotonously as the temperature is lowered. The measured signal due to electronic heating is linearly dependent on the used laser fluence. Comparing the temperature dependence of the measured τ_E with the predictions of the commonly accepted two-temperature model (TTM) in the perturbative regime showed a large discrepancy. The measured energy relaxation time is a factor of 2 higher than the calculated energy relaxation time at low temperatures (60 K).

We show that one of the most fundamental assumptions of the TTM is incorrect. Namely, the electron gas cannot attain a thermal distribution by e-e collsions on the picosecond time scale of the e-ph energy relaxation. We have demonstrated that the electron gas has a *non-thermal* distribution which results in an increase of the e-ph energy relaxation time with respect to the thermalized limit, i.e., the prediction of the TTM. With the new model that accounts for the e-e and e-ph dynamics simultaneously, good agreement with our measurements is achieved. We obtained the e-ph coupling constant and the e-e scattering rate for Ag and Au which are in agreement with other experimental and theoretical estimates.

Effects of e-e dynamics in laser-heated metals are best visible when the lattice temperature is held below room temperature and when the laser fluence is kept small. Under these conditions the heated electron distribution remains close to a degenerate distribution which causes the e-e collision rate to be greatly suppressed by the Pauli exclusion principle. The exceptionally sensitive time-resolved technique using surface-plasmon polaritons suits these conditions well.

APPENDIX: HOT-ELECTRON-INDUCED CHANGE OF THE DIELECTRIC CONSTANT

We will calculate the change of the dielectric constant of noble metals Ag and Au as a consequence of electronic heating. We will outline the derivation for Ag. The dielectric constant for frequencies in the visible contains three contributions: a Drude-like intraband term and two terms that account for interband transitions. The interband transitions are the transition from the filled d band to the Fermi level of the p conduction band (d-p) and the transition from the Fermi level of the p band to the empty s band (p-s). It is easily seen that the intraband part is largely insensitive to the heating of the electron gas. Namely, the average density of electrons is a constant and the Drude dephasing rate mainly depends on the phonon density. In the following we will focus on the d-p transition of Ag at 4.03 eV and adapt the model of Rosei *et al.*[25-27] The p-s transition and the case of Au can be treated similarly. First, we take a thermal electron distribution and later we will consider the nonthermal case.

The model of Rosei *et al.* accounts for the fact that the d-p transition is located near the L point (center of the neck) in the zone scheme. The band structure is assumed to have rotational symmetry along the Γ-L direction and parabolic bands characterized by the effective masses $m_{d\perp} = 2.58$, $m_{d\parallel} = 2.075$, $m_{p\perp} = 0.172$, and $m_{p\parallel} = 0.32$ (in units of the electron mass m_0). The d-p interband frequency is denoted by $\omega_{\rm inter}$ (4.03 eV). The imaginary part of the dielectric constant around the interband transtion is found to be

$$\epsilon''_{d-p}(\omega, T_e) = \frac{8\pi^2 e^2 \hbar^2}{3 m_0^2 \omega^2} |P(d \to p)|^2$$

$$\times \int \mathcal{D}_{d-p}(E, \omega)[1 - n(E, T_e)] dE, \quad (A1)$$

where $P(d \to p)$ is the transition matrix element and where the integral (= the joint density of states) contains the function $\mathcal{D}_{d-p}(E, \omega)$, which is called the energy distribution of the joint density of states. The latter quantity has the following proportionality:

$$\mathcal{D}_{d-p}(E, \omega) \propto \frac{\Theta\left[v_d \hbar(\omega - \omega_{\rm inter}) - E\right]}{\sqrt{v_d \hbar(\omega - \omega_{\rm inter}) - E}}. \quad (A2)$$

In this expression Θ is the Heaviside (step) function and $v_d \equiv m_{d\perp}/(m_{d\perp} + m_{p\perp}) = 0.89$.

We will focus on the electron-temperature-dependent part of the dielectric constant $\Delta\epsilon(\omega, T_e) = \epsilon(\omega, T_e) - \epsilon(\omega, 0)$. The Kramers-Kronig relations establish a connection between the real and imaginary parts of the dielectric constant. Since in order to calculate the total real part the imaginary part should be known over the whole spectrum, this method is generally difficult to apply. In the present case, however, the electron-temperature-dependent imaginary part is nonzero only within a small frequency interval around ω_{inter} so that the corresponding real part $\Delta\epsilon'_{d-p}$ can be easily derived:

$$\Delta\epsilon'_{d-p}(\omega_1, T_e) = \frac{2}{\pi}\mathcal{P}\int_0^\infty \frac{\omega\Delta\epsilon''_{d-p}(\omega, T_e)}{\omega^2 - \omega_1^2}d\omega, \quad (A3)$$

where $\mathcal{P}$ denotes the principal value of the integration. The obtained electron-temperature-dependent part of the real part is rewritten as

$$\Delta\epsilon'_{d-p}(\omega_1, T_e) \propto \int [n(E, T_e) - n(E, 0)]Z(E)dE, \quad (A4)$$

with

$$Z(E) = \frac{\pi}{2\omega_1^2}\sum_j \frac{a_j}{\sqrt{v_d\hbar(\omega_{\mathrm{inter}} - b_j\omega_1) + E}}, \quad (A5)$$

and $a_j = (1,1,-2)$, $b_j = (1,-1,0)$ for $j = 1$, 2, and 3. In our case where $\hbar\omega_1 = 2$ eV and $\omega_{\mathrm{inter}} = 2.5-4$ eV, the condition $k_B T_e \ll (\omega_{\mathrm{inter}} - \omega_1)$ is fulfilled and the function $Z(E)$ varies slowly around the Fermi level $E = 0$, so

that the Sommerfeld expansion[30] may be applied. In the Sommerfeld expansion, the function $Z(E)$ is expanded in a Taylor series around the Fermi level. The temperature-dependent term of the real part is

$$\Delta\epsilon'(\omega_1, T_e) \propto \frac{(k_B T_e)^2}{\omega_1^2}\left[\sum_j a_j\mathcal{L}_j(\omega_1)^{1/2} + \sum_j a_j\mathcal{L}_j(\omega_1)^{3/2}\right], \quad (A6)$$

with

$$\mathcal{L}_j(\omega_1) = \frac{E_F}{v_d\hbar(\omega_{\mathrm{inter}} - b_j\omega_1)}. \quad (A7)$$

The power-$\frac{1}{2}$ terms are due to the hot-electron- induced shift of the Fermi level (Fermi shift) and the power-$\frac{3}{2}$ terms are due to Fermi smearing. We find that the change of the real part of ϵ is proportional to the change of total thermal energy γT_e^2 of the electron gas.

The above derivation may be repeated for a nonthermal electron distribution, not far from the thermalized state. When the energy of the individual excitations (electrons and holes) and the probe photon energy are much smaller than the interband energy, the Sommerfeld expansion can be generalized resulting in the notion that the change of the dielectric constant is proportional to the total excess energy of electrons in the nonthermal distribution.

* Present address: Research Institute of Materials, Katholieke Universiteit Nijmegen, Toernooiveld 1, 6525 ED Nijmegen, The Netherlands. Electronic address: gveld@sci.kun.nl

[1] R. W. Schoenlein, W. Z. Lin, J. G. Fujimoto, and G. L. Eesley, Phys. Rev. Lett. **58**, 1680 (1987).

[2] H. E. Elsayed-Ali, T. B. Norris, M. A. Pessot, and G. A. Mourou, Phys. Rev. Lett. **58**, 1212 (1987).

[3] R. H. M. Groeneveld, R. Sprik, and A. Lagendijk, Phys. Rev. Lett. **64**, 784 (1990).

[4] S. D. Brorson, A. Kazeroonian, J. S. Moodera, D. W. Face, T. K. Cheng, E. P. Ippen, M. S. Dresselhaus, and G. Dresselhaus, Phys. Rev. Lett. **64**, 2172 (1990).

[5] S. G. Han, Z. V. Vardeny, K. S. Wong, O. G. Symko, and G. Koren, Phys. Rev. Lett. **65**, 2708 (1990).

[6] G. L. Eesley, J. Heremans, M. S. Meyer, and G. L. Doll, Phys. Rev. Lett. **65**, 3445 (1990).

[7] P. B. Allen, Phys. Rev. Lett. **59**, 1460 (1987).

[8] S. D. Brorson, W. Z. Lin, J. G. Fujimoto, and E. P. Ippen, Phys. Rev. Lett. **59**, 1962 (1987).

[9] P. B. Corkum, F. Brunel, N. K. Sherman, and T. Srinivasan-Rao, Phys. Rev. Lett. **61**, 2886 (1988).

[10] H. E. Elsayed-Ali, T. Juhasz, G. O. Smith, and W. E. Bron, Phys. Rev. B **43**, 4488 (1991).

[11] R. H. M. Groeneveld, R. Sprik, and A. Lagendijk, Phys. Rev. B **45**, 5079 (1992).

[12] W. S. Fann, R. Storz, H. W. K. Tom, and J. Bokor, Phys. Rev. Lett. **68**, 2834 (1992); Phys. Rev. B **46**, 13 592 (1992).

[13] C.-K. Sun, F. Vallée, L. Acioli, E. P. Ippen, and J. G. Fujimoto, Phys. Rev. B **48**, 12 365 (1993).

[14] G. Tas and H. J. Maris, Phys. Rev. B **49**, 15 046 (1994).

[15] C. A. Schmuttenmaer, M. Aeschlimann, H. E. Elsayed-Ali, R. J. D. Miller, D. A. Mantell, J. Cao, and Y. Gao, Phys. Rev. B **50**, 8957 (1994).

[16] M. Mihailidi, Q. Xing, K. M. Yoo, and R. R. Alfano, Phys. Rev. B **49**, 3207 (1994).

[17] C. R. Crowell and S. M. Sze, in *Physics of Thin Films* edited by G. Hass and R. E. Thun (Academic, New York, 1967).

[18] M. Kaveh and N. Wiser, Adv. Phys. **33**, 257 (1984).

[19] *Surface Polaritons*, edited by V. M. Agranovitch and D. L. Mills (North-Holland, Amsterdam, 1982).

[20] M. R. Philpott, J. Chem. Phys. **62**, 1812 (1975).

[21] J. P. Heritage, J. G. Bergman, A. Pinczuk, and J. M. Worlock, Chem. Phys. Lett. **67**, 229 (1979).

[22] J. E. Sipe and G. I. Stegeman, in *Surface Polaritons*, edited by V. M. Agranovitch and D. L. Mills (North-Holland, Amsterdam, 1982).

[23] E. Kretschmann, Z. Phys. **241**, 313 (1971).

[24] M.P. van Exter and A. Lagendijk, Phys. Rev. Lett. **60**, 49 (1988).

[25] R. Rosei, Phys. Rev. B **10**, 474 (1974).

[26] R. Rosei, Phys. Rev. B **10**, 484 (1974).

[27] R. Rosei, F. Antonangeli, and U. M. Grassano, Surf. Sci. **37**, 689 (1973).

[28] D. W. Pashley, Adv. Phys. **14**, 327 (1965).

[29] S. I. Anisimov, B. L. Kapeliovitch, and T. L. Perel'man, Zh. Eksp. Teor. Fiz. **66**, 776 (1974) [Sov. Phys. JETP **39**, 375 (1974)].

[30] N. W. Ashcroft and N. D. Mermin, *Solid State Physics* (Holt, New York, 1976).

[31] G. Grimvall, *The Electron-Phonon Interaction in Metals* (North-Holland, Amsterdam, 1981).

[32] *American Institute of Physics Handbook*, 2nd ed., edited by D. E. Gray (McGraw-Hill, New York, 1963).

[33] M. I. Kaganov, I. M. Lifshitz, and L. V. Tanatarov, Zh. Eksp. Teor. Fiz. **31**, 232 (1956) [Sov. Phys. JETP **4**, 173 (1957)] (Kaganov *et al.* define the Debye wave number k_0 according to $k_0^3 = \pi^3 n$, whereas the commonly used definition of the Debye wave number q_D is given by $q_D^3 = 6\pi^2 n$, where n is the density).

[34] In the high-temperature regime ≥ 60 K where the instantaneous relaxation time decreases as time progresses, $\tau_E(T_e(0), T_i)$ is an upper bound for the average relaxation time.

[35] *Numerical Data and Functional Relationships in Science and Technology*, edited by K.-H. Hellwege, Landolt-Börnstein, New Series, Group III, Vol. 15, Pt. a (Springer, Berlin, 1982), p. 14.

[36] G. Bergmann, Phys. Rev. B **3**, 3797 (1971).

[37] S. J. Poon and T. H. Geballe, Phys. Rev. B **18**, 233 (1978).

[38] B. Keck and A. Schmid, J. Low Temp. Phys. **24**, 611 (1976).

[39] D. Pines and P. Nozières, *The Theory of Quantum Liquids* (Benjamin, New York, 1966).

[40] J. J. Quinn, Phys. Rev. **126**, 1453 (1962).

[41] L. D. Landau and E. M. Lifshitz, *Physical Kinetics*, Vol. 10 of *Course on Theoretical Physics* (Pergamon, Oxford, 1981).

[42] D. Pines, *Elementary Excitations in Solids* (Benjamin, New York, 1963).

[43] J. L. Oudar, A. Migus, D. Hulin, G. Grillon, J. Etchepare, and A. Antonetti, Phys. Rev. Lett. **53**, 384 (1984).

[44] J. L. Oudar, D. Hulin, A. Migus, A. Antonetti, and F. Alexandre, Phys. Rev. Lett. **55**, 2074 (1985).

[45] T. Elsaesser and J. Shah, Phys. Rev. Lett. **66**, 1757 (1991).

[46] A. J. F. Levi, J. R. Hayes, P. M. Platzman, and W. Wiegman, Phys. Rev. Lett. **55**, 2071 (1985).

[47] A. F. J. Levi, Electron. Lett. **124**, 1273 (1988).